Chemical Engineering Communications

ISSN: (Print) (Online) Journal homepage: https://www.tandfonline.com/loi/gcec20

Evaluation of Crocin as green corrosion inhibitor for aluminum in NaCl solution

Paraskevi Pantazopoulou, Sofia Kalogeropoulou, Stamatina Theohari, Eleftherios Papamichalis & Demeter Tzeli

To cite this article: Paraskevi Pantazopoulou, Sofia Kalogeropoulou, Stamatina Theohari, Eleftherios Papamichalis & Demeter Tzeli (2023) Evaluation of Crocin as green corrosion inhibitor for aluminum in NaCl solution, Chemical Engineering Communications, 210:10, 1756-1772, DOI: 10.1080/00986445.2022.2147834

To link to this article: https://doi.org/10.1080/00986445.2022.2147834

CHEMICAL ENGINEERING COMMUNICATIONS
2023, VOL. 210, NO. 10, 1756–1772
https://doi.org/10.1080/00986445.2022.2147834

Evaluation of Crocin as green corrosion inhibitor for aluminum in NaCl solution

Paraskevi Pantazopoulou[a], Sofia Kalogeropoulou[a], Stamatina Theohari[b], Eleftherios Papamichalis[c,d], and Demeter Tzeli[c,d]

[a]Department of Electrical and Electronic Engineering, University of West Attica, Egaleo, Athens, Greece; [b]Graphic Design and Visual Communication Department, University of West Attica, Egaleo, Athens, Greece; [c]Laboratory of Physical Chemistry, Department of Chemistry, National and Kapodistrian University of Athens, Zografou, Greece; [d]Theoretical and Physical Chemistry Institute, National Hellenic Research Foundation, Athens, Greece

ABSTRACT

The role of Crocin, which is a natural organic substance from the Greek plant *Crocus sativus*, is investigated as a green corrosion inhibitor for the AA 1050 commercial aluminum alloy in 0.01 M sodium chloride solution. Its action was assessed by Linear and Tafel Polarization, as well as by mass loss measurements and confirmed by observation and analysis of the surface morphology of the specimens by Scanning Electron Microscopy. Corrosion inhibition efficiency of Crocin improves with concentration and at 1.25 mM was estimated in the range of 90-95%, which indicates the formation of an adsorbed layer that isolates and protects the surface. Experimental results showed that Crocin acts as a mixed-type inhibitor with predominantly anodic effectiveness, also retarding pitting corrosion process. The inhibitive action of Crocin was explained by theoretical calculations employing density functional theory, semiempirical PM6 and molecular mechanics methodologies, showing good agreement with experimental results. The reactivity of Crocin is attributed to chemisorption on the Al_2O_3 surface through its vicinal hydroxyls of the sugar moiety. This process is assisted by the π-conjugated system of the polyene chain together with the extended electron delocalization over the oxygen atoms of the esterified carboxyl groups, as well as by the intense electrostatic potential regions located on the sugar moiety of the Crocin molecule.

KEYWORDS

Aluminum corrosion inhibitors; Crocin; density functional theory; electrochemical techniques; PM6; theoretical calculations

1. Introduction

Aluminum alloys are widely used in various applications, including packaging, construction, shipbuilding, and automotive and aerospace industry, due to their low cost and interesting properties of lightweight, ductility, durability, and recyclability. Besides, aluminum is resistant to corrosion, as a very thin passive oxide layer of about 1-3 nm develops spontaneously on its surface when it is exposed to air or to aqueous environment. This layer consists of Al_2O_3, $Al(OH)_3$, AlO·OH, and their hydrous forms, with certain oxyhydroxides present in the bulk of the aluminum oxide. The hydration of the surface is followed by dissociation and ionization, leading to the formation of $[Al(OH)_2]^+$ or $AlO{\cdot}O^-$ (Alexander et al. 2000; Lee and Pyun 1995; Sheasby et al. 1987).

Depending on the pretreatment and the environment, several morphological characteristics of the aluminum oxide are influenced, such as surface density, homogeneity and porosity, number, volume and distribution of pores, vacancies or defects. This surface exhibits an amphoteric character, presenting zero charge in neutral solutions, positive in acidic and negative in alkaline conditions, thus influencing its chemical reactivity (Kasprzyk-Hordern 2004; Kummert and Stumm 1980). So, despite the passivation of aluminum, the outer surface of the naturally formed oxide is susceptible and permeable to aggressive ions when exposed to various severe conditions, leading to depassivation and corrosion phenomena. Especially in chloride solutions, Cl^- ions attack and damage the oxide layer in certain sites resulting in pitting corrosion (Ambat and

CONTACT Paraskevi Pantazopoulou parpant@uniwa.gr; Stamatina Theohari stheochari@uniwa.gr; Demeter Tzeli tzeli@chem.uoa.gr

Dwarakadasa 1994; Ezuber et al. 2008; Ma 2012; McCafferty 2003; Murer and Buchheit 2013; Natishan and O'Grady 2014; Szklarska-Smialowska 1999; Xhanari and Finsgar 2019).

Corrosion inhibition for aluminum protection in aggressive environments has been extensively investigated (Aytaç et al. 2005; Byrne et al. 2022; Fouda et al. 2009; Garrigues et al. 1996; Maayta and Al-Rawashdeh 2004). Organic compounds, especially those containing polar groups with N, O, S atoms etc. in conjugated molecular systems, present inhibition efficiency determined by their electron density and their contribution to electron acceptance or donation processes (Branzoi et al. 2003; Kliškić et al. 1997; Önal and Aksüt 2000; Rosliza et al. 2010). Their action is attributed to their affinity to interact and be adsorbed on the aluminum surface forming protective layers (El Mazyani et al. 2021; Giles 1974; Oguzie et al. 2006, 2010; Pantazopoulou et al. 2021; Theohari et al. 2015; Tirbonod and Fiaud 1978; Tsangaraki-Kaplanoglou et al. 2010). However, many of these compounds have been questioned due to their toxicity and negative effects on the environment and ecosystems. Natural substances of plant origin and pharmaceutical compounds have gained significant attention as eco-friendly and safe for human health corrosion inhibitors (Abdallah et al. 2020; Abdallah et al. 2021; Abdallah et al. 2022; Amitha Rani and Basu 2012; Ashassi-Sorkhabi and Kazempour 2020; Byrne et al. 2022; Carneiro et al. 2015; El-Etre 2003; Fernine et al. 2021; Kasprzyk-Hordern 2004; Lai et al. 2021; Luo et al. 2019; Müller 2002; Oguzie 2007; Proença et al. 2022; Raja and Sethuraman 2008; Sangeetha et al. 2013; Solmaz et al. 2008; Umoren et al. 2018; Verma et al. 2018, 2021; Nik et al. 2012; Xhanari et al. 2017; Zhang et al. 2018).

In order to understand and describe the role of organic molecules on the corrosion inhibition of aluminum, quantum chemical methods have been used recently in addition to electrochemical experimental methods (Becke 1993; Costa et al. 2016; Curtiss et al. 1995; Dapprich et al. 1999; Lee et al. 1988; Martinez and Štagljar 2003; Nakashima 2018; Obot et al. 2015; Pearson 1993; Rakshit et al. 2019; Rappé et al. 1992; Rocher-Casterline et al. 2011; Spencer and Nyberg 2002; Stewart 2007; Tsirelson et al. 1985; Tzeli et al. 2002; Vreven and Morokuma 2006). Researchers use Density Functional Theory (DFT) to calculate the minimum energy structures, geometries, highest occupied molecular orbital (HOMO), lowest unoccupied molecular orbital (LUMO), as well as dipole moment (μ) of the inhibiting molecules, and thus to correlate their stability and inhibition reactivity based on the values of Energy gap (E_L–E_H) and hardness (η), which is expressed in terms of ionization potential (I) and electron affinity (A) of the molecules as $\eta = (I - A)/2$ or $\eta = (E_L–E_H)/2$ (De Proft and Geerlings 2001; Kathirvel et al. 2014; Omelchenko et al. 2011). These theoretical studies are also useful for designing new systems of corrosion inhibitors. For this purpose, certain quantum parameters should be taken into consideration, since high E_H values are related to the capacity of a molecule to donate electrons to an appropriate acceptor (i.e., aluminum oxide), which facilitates the adsorption process and therefore indicates a better behavior of the corrosion inhibitor. Low E_L values correspond to a tendency for electron acceptance, usually from the metal surface atoms, while the energy difference between E_L and E_H is indicative of the inherent electron donating ability of the inhibitor and represents its efficiency to interact with the metal surface.

In the present study Crocin ($C_{44}H_{64}O_{24}$), which is a nontoxic substance of plant origin contained in the stems of the plant *Crocus Sativus*, with no impact on human life and the environment, is investigated against the corrosion of the commercial pure aluminum alloy AA1050 in the aggressive environment of chloride ions at room temperature. Crocin is one of the few natural carotenoids easily soluble in water, that has been reported not only as coloring matter in food and textile industry but also as an effective antioxidant, anticarcinogenic and neuroprotective agent in drugs and nutritional supplements (Bathaie et al. 2014; Cerdá-Bernad et al. 2022; Soror 2013; Rahaiee et al. 2015; Tsangaraki-Kaplanoglou et al. 1989; Yan et al. 2021). Its reactivity is attributed to the presence of active centers in its chemical structure. Therefore, Crocin is expected to be a promising eco-friendly corrosion inhibitor. Potentiodynamic electrochemical

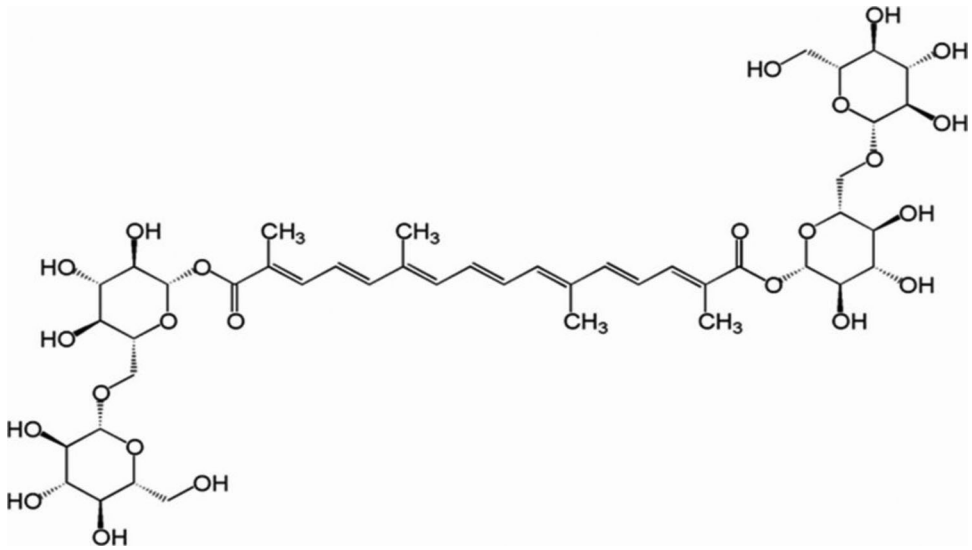

Figure 1. Molecular structure of Crocin (8,8-diapo-8,8-carotenoid acid).

techniques, mass loss measurements and Scanning Electron Microscopy were employed to elucidate the action of Crocin toward the corrosion of aluminum. Experimental findings were completed and verified using computational methods, i.e., density functional theory (DFT), semiempirical PM6, molecular mechanics (MM) simulations and multiscaling ONIOM (DFT/PM6) and ONIOM (DFT/MM) approaches.

2. Materials and methods

2.1. Experimental part

Specimens of AA1050 commercial aluminum alloy with >99% Al were used, having nominal composition (% by weight): 0.168 Si − 0.245 Fe − 0.003 Mn − 0.001 Mg − 0.001 Cu − 0.006 Ti − 0.002 Cr − 0.013 Zn. Coupons of 20 mm × 20 mm × 0.5 mm were mechanically polished, cleaned and stored in desiccator until their use.

The corrosive medium was 0.01 M NaCl solution prepared by NaCl p.a. and deionized water. The inhibitor was Crocin or 8,8-diapo-8,8-carotenoid acid, which is a diester of the disaccharide gentiobiose and the dicarboxylic acid crocetin (Figure 1). It was supplied from Sigma-Aldrich, and was added in various concentrations in the NaCl solution.

The electrochemical behavior of the AA1050 specimens in the testing solutions was investigated by Potentiodynamic Polarization techniques, performed at room temperature by a Gamry Interface 1000 and DC105 Corrosion Software using a three-electrode cell setup. The reference electrode was Ag/AgCl, the counter electrode was Pt and the surface area of the AA1050 working electrode in contact with the electrolyte was 1 cm^2. Open Circuit Potential (OCP) was recorded for 60 min until an almost steady value was reached. Linear Polarization was carried out at a scan rate of 0.125 mV/s and Tafel Scan was performed at a scan rate of 0.166 mV/s.

Polarization resistance (R_p) was determined from Linear Polarization curves. The inhibition efficiency of solutions containing Crocin was calculated from corrosion currents derived from Tafel curves by the equation:

$$IE\ (\%) = \left[(I_{corr,B} - I_{corr,S})/I_{corr,B}\right] \times 100 \qquad (1)$$

where $I_{corr,B}$ and $I_{corr,S}$ are the corrosion currents in the blank and inhibiting solutions, respectively.

Mass loss measurements were performed for a total period of 9 weeks. Aluminum specimens were immersed in the examined solutions at room temperature and were weighed weekly after cleaning according to ISO 8407. From these measurements, inhibition efficiency of Crocin was also calculated using the equation:

$$IE\ (\%) = \left[(\Delta m_{corr,B} - \Delta m_{corr,S})/\ \Delta m_{corr,B}\right] \times 100 \qquad (2)$$

where $\Delta m_{corr,B}$ and $\Delta m_{corr,S}$ are the mass loss

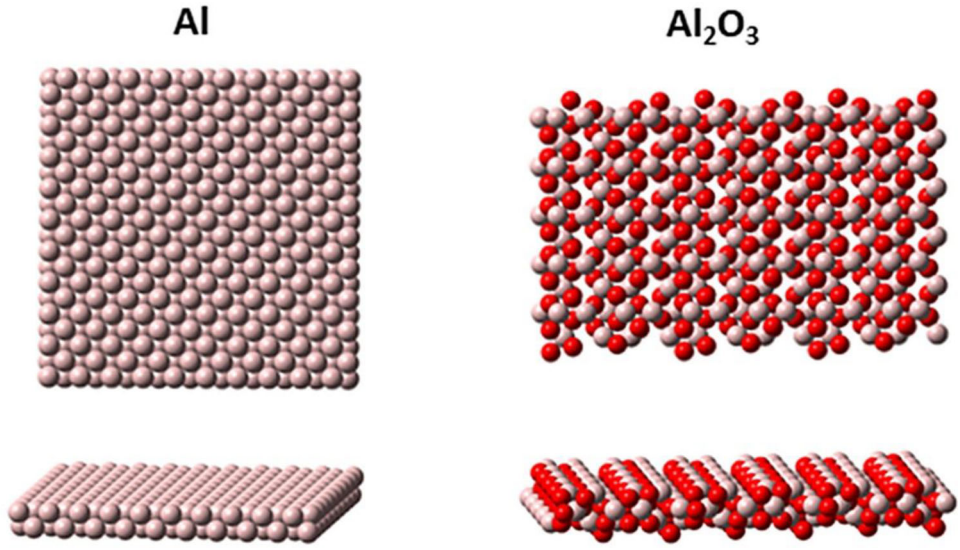

Figure 2. Calculated structures of Al(110) and Al_2O_3 surfaces from two points of view.

values in the blank and inhibiting solutions, respectively.

Observation and analysis of the specimens' surface was carried out by Scanning Electron Microscopy (SEM) (JEOL JSM-6510 LV).

2.2. Computational part

In order to study theoretically the possible interactions between the aluminum/aluminum oxide layer and the Crocin molecules in the aggressive environment, a computational analysis was performed on Al(110) and Al_2O_3 surfaces (Figure 2). Given that the real surface in a naturally formed aluminum oxide layer is very thin and expected to have a rather inhomogeneous morphology with discontinuities, pores, vacancies or defects, Al and Al_2O_3 surfaces were both investigated in the presence of Crocin, Cl^- anions, Na^+ cations and O_2 molecules, all of which are present in the experimental procedure.

A model cluster of Al comprising of 340 atoms and model clusters of Al_2O_3 having 450 and 1050 atoms were used, fixed at the known experimental geometries (Nakashima 2018; Tsirelson et al. 1985). The use of model cluster calculations has been shown to successfully describe the properties of the adsorbate-substrate system with excellent agreement with experimental observations (Spencer and Nyberg 2002). In this study, two Al_2O_3 model clusters were used for comparison reasons. For the Al model, a cubic cell with $a = 4.0339$ Å (space group, Fm-3m) (Nakashima 2018) was used and for the Al_2O_3 an hexagonal cell was used with cell parameters 4.7606 Å; 4.7606 Å; 12.994 Å (space group, R-3c:H) (Nakashima 2018; Tsirelson et al. 1985). The interaction of Crocin with Al and Al_2O_3 was calculated via molecular mechanics (MM) using the universal force field (UFF) (Rappé et al. 1992), via semi-empirical PM6 method (Stewart 2007) and density functional theory (DFT) using the B3LYP (Becke 1993; Lee et al. 1988) functional in conjunction with the 6-31 G(d,p) and 6-311 + G(d,p) basis sets (Curtiss et al. 1995). Moreover, the ONIOM methodology (Dapprich et al. 1999; Vreven and Morokuma 2006) was employed, where the calculated systems were defined as two regions (layers). The high layer consists of Crocin calculated at the B3LYP/6-31G(d,p) and B3LYP/6-311 + G(d,p) level of theory and the low layer is the model cluster calculated at the MM or PM6 level of theory. The binding energies (BE) were calculated via the equation:

$$BE = E_{surface-Crocin} - E_{surface} - E_{Crocin} \quad (3)$$

where, $E_{surface\text{-}Crocin}$, $E_{surface}$, and E_{Crocin} are the absolute energies of the complex system surface-Crocin, of the surface and of the Crocin molecule, respectively. Note that negative values of BE mean stable structures. All calculations were done using the gaussian16 program (Gaussian 16, Frisch et al. 2016).

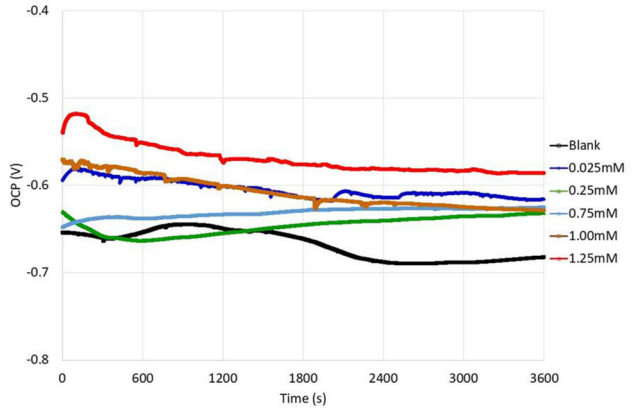

Figure 3. Open Circuit Potential (OCP) curves of AA1050 alloy in 0.01 M NaCl in the presence or absence of Crocin vs. time.

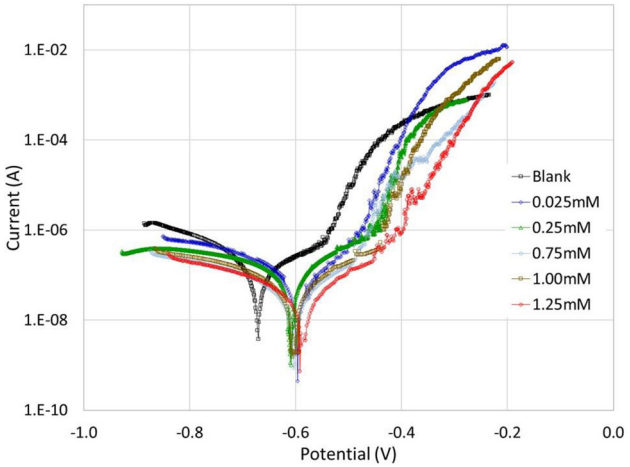

Figure 4. Potentiodynamic polarization curves for AA1050 test specimens immersed in 0.01 M NaCl in the presence or absence of Crocin.

3. Results and discussion

3.1. Electrochemical studies

Variation of the Open Circuit Potential (OCP) with immersion time of the AA1050 specimens in the 0.01 M NaCl blank solution and in the solutions where Crocin was added in the examined concentrations is presented in Figure 3. OCP is stabilized and an almost steady state condition is reached in all cases after one hour of exposure. In particular in the blank solution, OCP decreases initially due to the attack by the chloride ions, then increases slightly possibly because of the formation of a thin passive oxide layer on the aluminum surface and finally decreases again because of the corrosion reactions in the corrosive environment. In the case of the Crocin-containing solutions, OCP values are more positive, in the region of −630 to −590 mV, compared to the value in the blank solution (-680 mV) indicating a possible protective action of Crocin molecules. Moreover, as the most positive value of OCP, equal to −590 mV, was obtained with the concentration of 1.25 mM of Crocin, the best inhibition effect is expected to occur in this case.

Electrochemical data of aluminum specimens in the examined solutions, i.e., corrosion potential, corrosion current, Tafel anodic and cathodic slopes, corrosion rate and pitting potential, determined from Tafel polarization curves displayed in Figure 4, are given in Table 1. Polarization resistance (R_p) values obtained from Linear Polarization curves are also presented.

It is observed that the corrosion potential (E_{corr}) in the inhibitor-containing solutions is shifted toward more anodic values relatively to the E_{corr} in the blank solution. This shift is suggestive of the anodic inhibitive action of Crocin suppressing aluminum dissolution reaction. This is confirmed by the decrease in the anodic Tafel constant (β_a) as the concentration of Crocin increases. However, as the shift of E_{corr} in the presence of the inhibitor is slight and lower than 85 mV (Verma et al. 2021) it could be suggested that Crocin has an inhibiting effect on cathodic reactions as well (Byrne et al. 2022; Fouda et al. 2009; Xhanari and Finsgar 2019). The observed slight decrease in the cathodic Tafel slope (β_c) confirms the mixed-type inhibiting action of Crocin, but as the decrease in the anodic Tafel constant (β_a) is more significant, the anodic inhibiting action of Crocin must be predominant (El Mazyani et al. 2021; Fernine et al. 2021; Lai et al. 2021; Verma et al. 2021).

The decrease in the corrosion currents, combined with the increase in the R_p values, as well as the significant decrease in the corrosion rate (CR) as the concentration of Crocin in the sodium chloride corrosive solution increases, indicate also the protective action of Crocin. Indeed in the case of the 1.25 mM Crocin solution R_p value is almost five times higher compared to that in the blank solution, while the corresponding CR value is almost ten times lower.

The inhibition efficiency of the solutions with Crocin calculated from corrosion currents is

Table 1. Electrochemical data of AA1050 test specimens immersed in 0.01 M NaCl in the presence or absence of Crocin in various concentrations.

Crocin (mM)	E_{corr} (V)	I_{corr} (A)	β_a (V/dec)	β_c (V/dec)	CR (mpy)	E_{pit} (V)	R_p (kOhm)
Blank	−0.671	7.12E − 07	0.932	0.498	0.309	−0.540	210
0.025	−0.596	2.19E − 07	0.314	0.467	0.094	−0.500	375
0.25	−0.604	1.96E − 07	0.292	0.456	0.085	−0.460	390
0.75	−0.603	1.30E − 07	0.270	0.452	0.056	−0.450	715
1.00	−0.604	1.36E − 07	0.265	0.449	0.058	−0.440	832
1.25	−0.587	7.44E − 08	0.261	0.450	0.032	−0.420	980

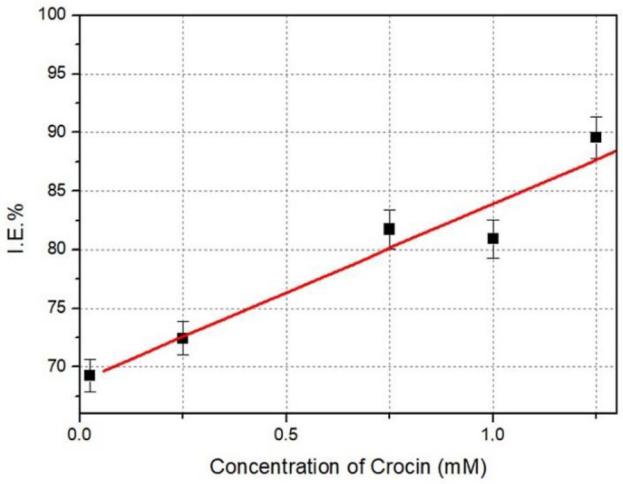

Figure 5. Inhibition efficiency (%) of test solutions obtained from corrosion currents.

presented in Figure 5 as a function of its concentration. All values are high, varying from 70% to 90% and the highest values are obtained with the 1.25 mM solution. These values predict interaction of Crocin molecules with the substrates and coverage of a large part of the Al and Al_2O_3 surfaces available for corrosion reactions, by forming a natural protective organic film with high chloride blocking capacity in the experimental conditions. This inhibiting action is attributed to the molecular structure of Crocin. The distribution of active electrons in the Crocin molecule through extended delocalization in the -C = C- bonds of the central unsaturated chain of the molecule and the esterified carboxyl groups could play a significant role, as mentioned by Akhtari et al. (2013). Moreover, the most intense electrostatic potential regions located on the two groups of gentiobiose terminals of the molecule may also contribute to its reactivity, as will be explained below.

It is noteworthy that a shift of pitting corrosion potential (E_{pit}) with the concentration of Crocin toward less negative values is observed, from −540 mV in the blank solution to −420 mV in the 1.25 mM inhibiting solution (Table 1). E_{pit} is the potential below which the metal surface remains passive and it is determined from the anodic branch of the Tafel curves (Figure 4) as the potential where the current increases sharply. Above this potential, pitting corrosion on the surface starts. As mentioned in the literature, in NaCl solutions without inhibitors (Ambat and Dwarakadasa 1994; Branzoi et al. 2003), Cl^- ions are attracted to the surface, adsorb and penetrate into the natural passive oxide film, breaking it and accelerating pitting corrosion. In addition, repassivation of the surface is delayed due to oxygen reduction, which causes local increase in pH and formation of aluminate ions (AlO_2^-) (Oguzie et al. 2010). The presence of Crocin blocks the pitting corrosion process as its molecules interact with Al/Al_2O_3 surface, leading to rapid repassivation of the surface as soon as pitting corrosion starts. Therefore, it can be concluded that Crocin modifies the characteristics and properties of the surface, making it more stable against the corrosive environment of chloride ions.

3.2. Mass loss measurements

Mass loss of the AA1050 specimens vs. immersion time (Figure 6a), as well as vs. concentration of Crocin (Figure 6b) was determined. The anticorrosive action of Crocin is evident, especially at the concentration of 1.25 mM where the calculated inhibition efficiency reached 95%. These results are in good agreement with the findings derived from the electrochemical measurements, confirming the drastic reduction of the anodic dissolution reaction due to the formation of a protective film with blocking capacity against the chloride ions present in the solution.

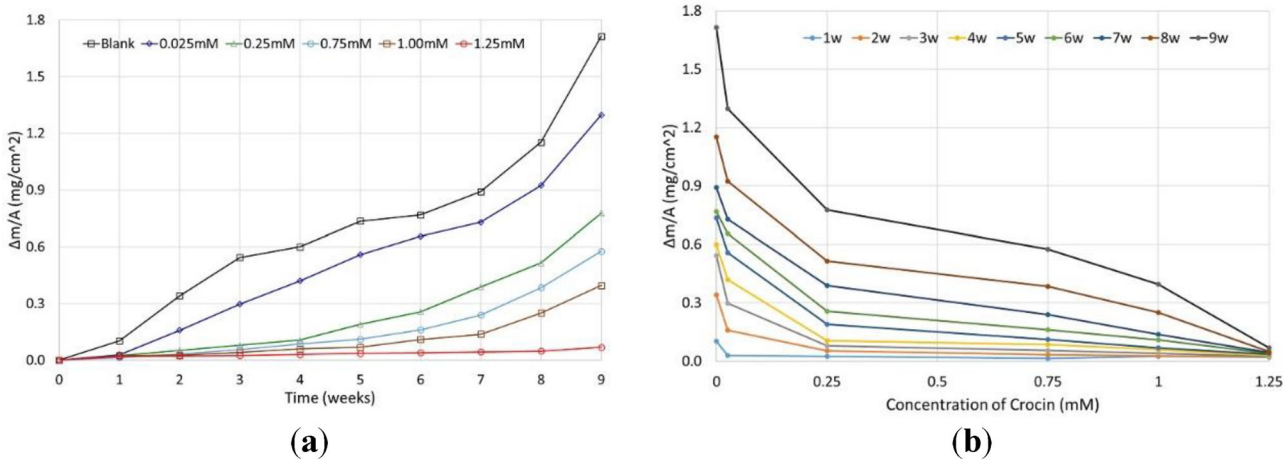

Figure 6. Mass loss of the AA1050 specimens (a) vs. immersion time and (b) vs. concentration of Crocin for 1 to 9 weeks of immersion.

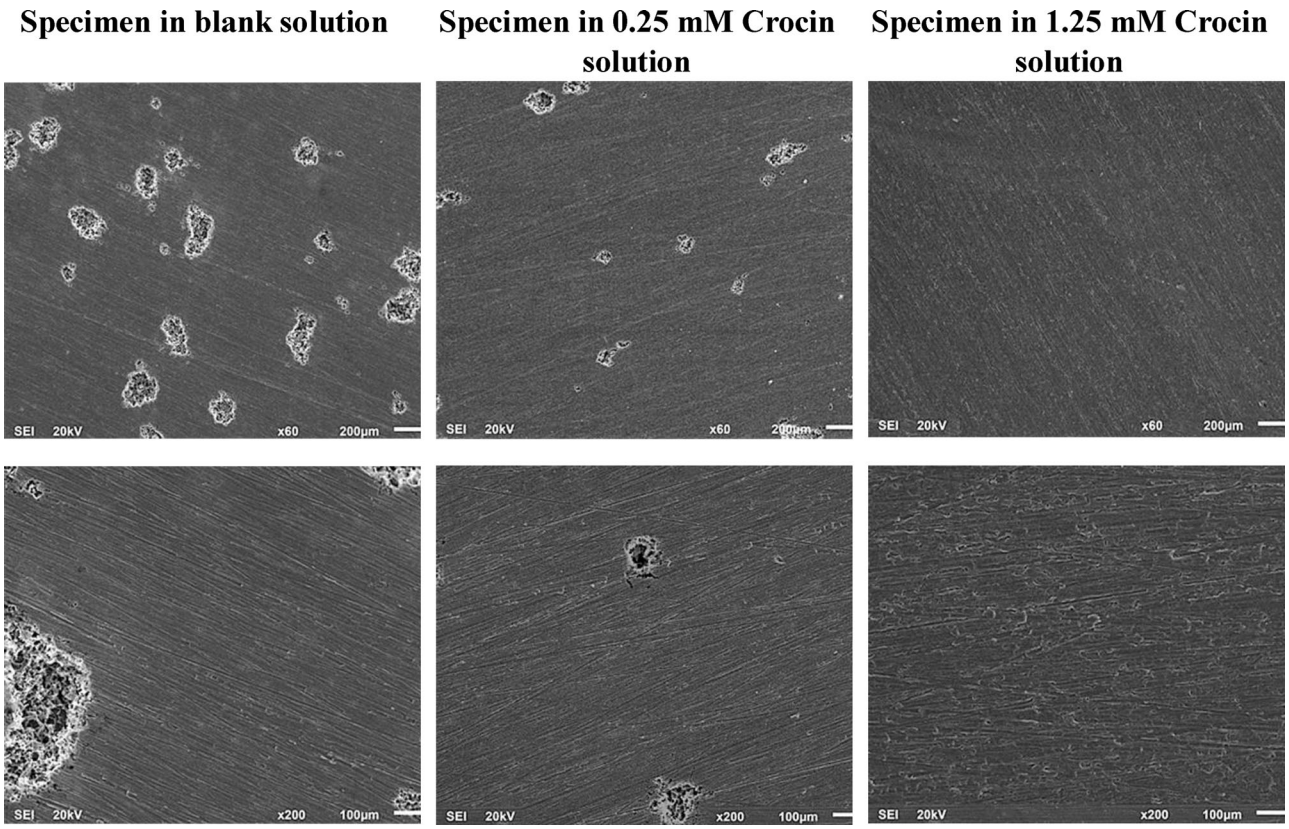

Figure 7. SEM micrographs (X60 and X200) of AA1050 surfaces after polarization tests in 0.01 M NaCl in the presence or absence of Crocin.

3.3. Surface morphology of the specimens

Surface morphology of the AA1050 specimens, before and after the electrochemical corrosion tests, was studied by SEM. The images shown in Figure 7 represent the micrographs of the specimens after the tests at X60 and X200 magnifications. Less corrosion spots are present on the surface as the concentration of Crocin in the solutions increases. The color of the specimens immersed in the blank solution is darker and their surface exhibits a porous-like morphology. The specimens immersed in the Crocin-containing solutions show a generally less corroded and smoother surface, with less pores and holes.

Particularly in the case of 1.25 mM Crocin solution, signs of localized spots of pitting corrosion are not detected. These results confirm the beneficial effect of Crocin as corrosion inhibitor and corroborate the findings of the electrochemical corrosion tests and mass loss measurements.

3.4. Theoretical calculations

Experimental findings of the protective role of Crocin as a mixed type inhibitor against aluminum corrosion in sodium chloride solutions were interpreted and evaluated by theoretical calculations, in order to further investigate the relationship between the molecular structure of Crocin and its inhibiting action. The interaction of Crocin with aluminum and the physically formed aluminum oxide surfaces, as well as the inhibition action of Crocin against the action of Cl^- anions, were theoretically evaluated.

Crocin molecule: At first, conformation analysis of Crocin was carried out in order to find the lowest in energy minima structures (Figure 8). They are near energetically degenerate, i.e., they are very close in energy. Their energy differences (ΔE) are within 0.2 eV (Table 2). As a result, all these minima structures are present when Crocin is free in aqueous environment, as happens under the experimental conditions of the present study. The minima have been named with respect to the relative positions of the two gentiobiose

Table 2. Relative energies ΔE (eV), dipole moments μ (debye), Energy difference of HOMO-LUMO orbitals E(H-L) (eV) and hardness η (eV) at B3LYP/6-31G(d,p) and B3LYP/6-311 + G(d,p) of the four lowest in energy minima of Crocin.

Conformer	ΔE	μ	E(H-L)	η
	B3LYP/6-31G(d,p)			
TC	0.00	4.339	2.451	1.225
P1C	0.06	3.417	2.453	1.226
P2C	0.11	1.903	2.456	1.228
TT	0.25	3.687	2.446	1.223
	B3LYP/6-311 + G(d,p)			
TC	0.00	4.436	2.418	1.209
P1C	0.05	3.503	2.421	1.210
P2C	0.09	1.872	2.425	1.212
TT	0.21	3.489	2.415	1.208

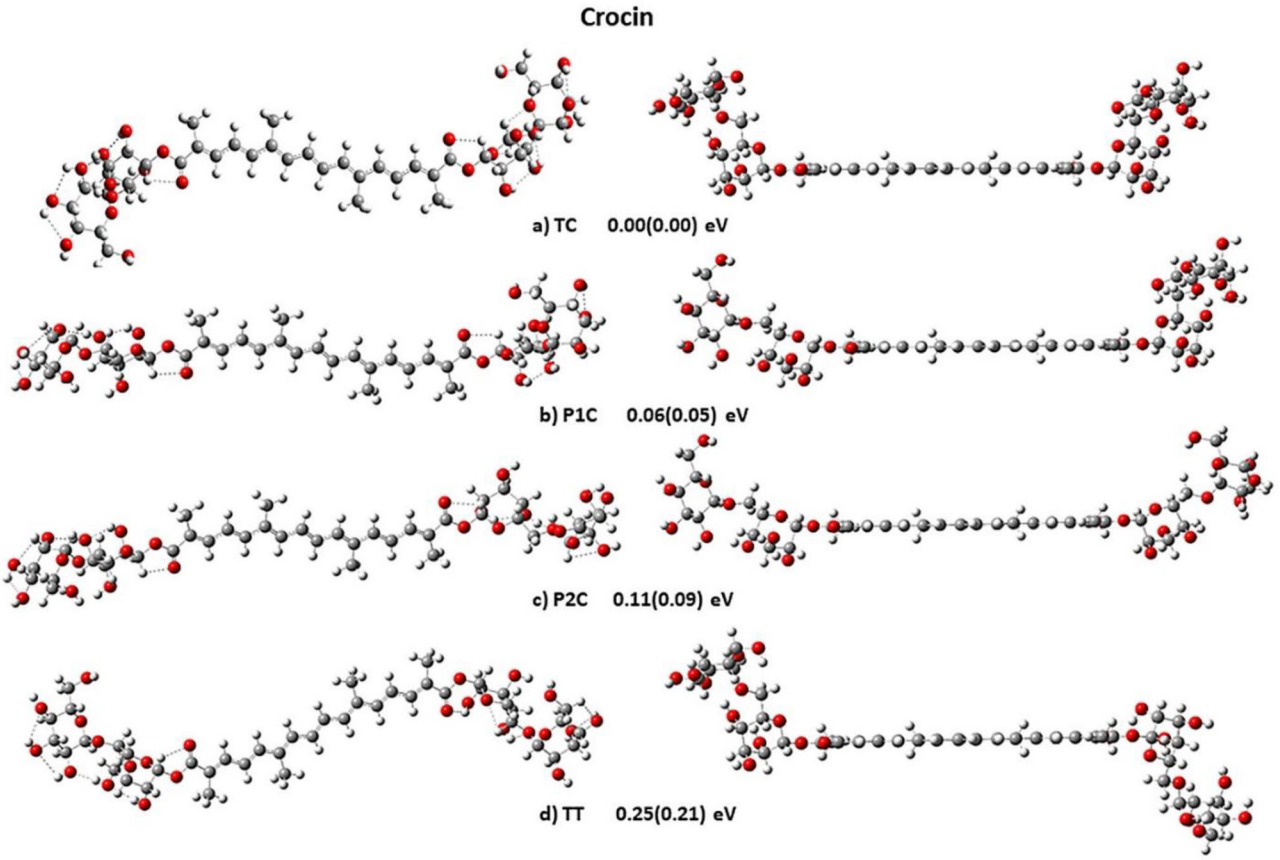

Figure 8. Calculated minimum structures of the four lowest in energy isomers of Crocin molecule from two points of view. Intramolecular hydrogen van der Waals bonds are shown. Relative energies at B3LYP/6-31G(d,p) (B3LYP/6-311 + G(d,p)).

Table 3. van der Waals distances RH … O (Å), number of van der Waals bonds (vdW) and dipole moments μ (debye) at B3LYP/6-311 + G(d,p) of the four lowest in energy minima of Crocin and of the physisorbed Crocin on Al(110) and Al_2O_3 surfaces.

Conformer	RH … O	vdW	M
TC	1.912–2.440	11	4.436
P1C	1.913–2.433	10	3.505
P2C	1.913–2.442	10	1.872
TT	1.915–2.431	10	3.489
on Al(110)	2.148–2.550	7	2.191–3.743
on Al_2O_3	1.970–2.495	8	9.169–9.262

groups. They are labeled with two letters, the first one with respect to the plane of the alkene chain and the second one with respect to the plane perpendicular to the alkene chain (Figure 8), i.e., T for trans, C for cis and P for plane.

As expected, van der Waals bonds (vdW) are formed between the hydrogen atoms of the OH or CH_2 and the O atoms (Figure 8). Ten or eleven such bonds are formed with bond distances that range from 1.91 to 2.44 Å (Table 3). Note that when Crocin is physisorbed on Al and Al_2O_3 surfaces, less vdW intra-interactions are formed, i.e., the number of bonds is reduced to eight or seven with elongated bond distances because Crocin interacts with the surface, as explained below.

The four calculated conformers differ in their dipole moments, i.e., their values range from 1.87 to 4.44 debye due to the different relative positions of the glucose rings and of the OH of the gentiobiose groups. These differences could probably be related to the different effectivity regarding adsorption of the conformers. This fact may be attributed to the extended delocalization due to the distribution of active electrons through the -C = C- groups in the polyene chain. Besides, the intense electrostatic potential regions located on the sugar moiety of Crocin could play a significant role (Akhtari et al. 2013). However, the calculated energy difference of frontier HOMO and LUMO orbitals, E(H-L), and the hardness, η, (De Proft and Geerlings 2001; Omelchenko et al. 2011) have the same values for all four minima in both levels of theory (Table 2), indicating that all conformers exhibit similar reactivity. Note that easy transitions occur from one minimum to another due to low rotational C-C barrier (Figure 8). Finally, it should be noted that the relative direction of the rings in the two gentiobiose groups of the molecule possibly allow the formation of inter- and intramolecular attractions between the molecules through H bonds and van der Waals forces.

Crocin on surfaces: When Crocin is in contact with the Al(110) and Al_2O_3 surfaces, it deforms its minimum geometry in order to obtain a planar form and to increase its interaction with the surface (Figure 9). This interaction due to physisorption (weak forces) or chemisorption (electrostatic/ionic or covalent bonds) is expected to influence the effectiveness of the corrosion inhibitor. Specifically, van der Waals and hydrogen bonding due to the numerous vicinal hydroxyl groups of Crocin are expected to allow loose attachment to the surface to occur. Inter- and intramolecular forces between hydroxyl and carbonyl groups of the molecules are related also with the direction and orientation of the terminal rings of Crocin and influence its planar-type lying onto the surface. The chemical interactions, i.e., covalent and ionic/electrostatic bonds, are crucial for the formation of a stable protective layer of Crocin molecules on the surface in the aggressive aqueous environment. The extended delocalization due to the distribution of active electrons in Crocin molecule must be of great importance, as previously mentioned. The intense electrostatic potential regions located on the gentiobiose groups of Crocin (Akhtari et al. 2013) could be the anchoring groups onto the positively charged passivated aluminum surface, due to the weakly acidic environment in the present experimental conditions.

Physisorption: As mentioned above, Crocin deforms its geometry to obtain a planar form and to increase its interaction with the surface. The energy difference between the deformed planar adsorbed Crocin structure and the global minimum structure TC is 0.6 eV, which is due to the interactions between Crocin and surfaces. Specifically, Crocin forms vdW OH … O on Al_2O_3 and O … Al on Al and electrostatic interactions with the surfaces. The bond distances are about 2.4 Å on Al_2O_3 and 3.1 Å on Al surfaces (Figure 9). It is of interest that the physisorbed Crocin on the Al_2O_3 and Al surfaces forms less vdW intra interactions, i.e., seven or eight with

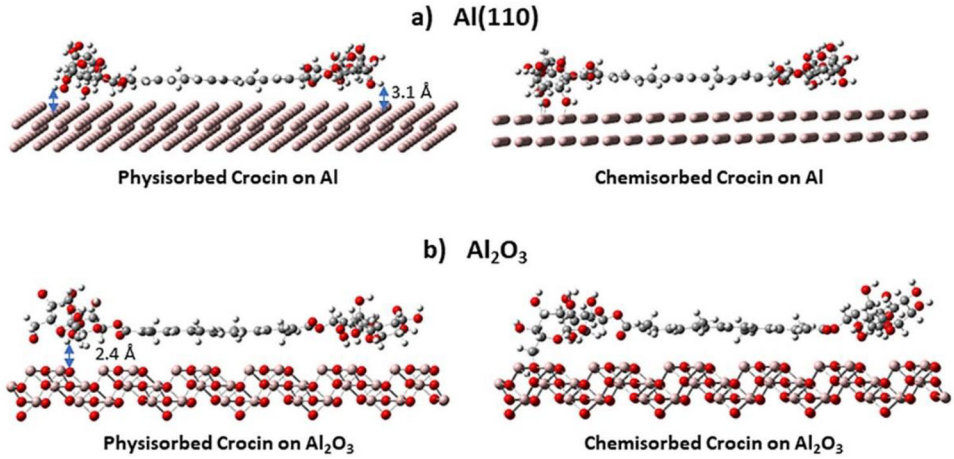

Figure 9. Calculated minimum structures of physisorbed and chemisorbed Crocin molecule on Al(110) and Al_2O_3 surfaces.

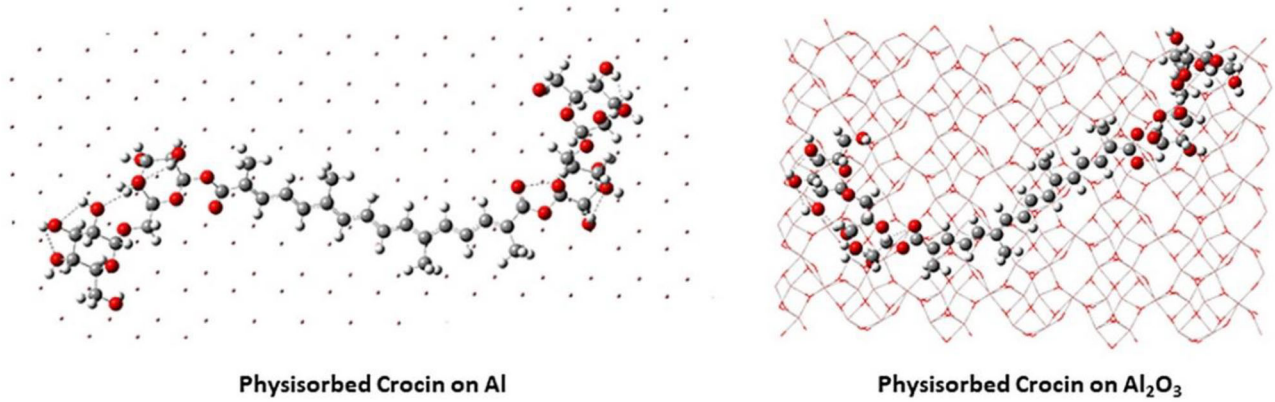

Figure 10. Intramolecular hydrogen van der Waals bonds of Crocin are shown.

elongated bond distances up to 0.2 Å with respect to the free one, because Crocin interacts with the surface (Table 3 and Figure 10). Furthermore, a significant increase in its dipole moment is observed on Al_2O_3 at 9.169-9.262 debye in comparison with that on Al(110), which is 2.191-3.743 debye. This means that more intense electrostatic interactions are formed on Al_2O_3, and thus Crocin is turned to an electric dipole.

As shown in Figure 11, in the case of physisorption, the molecular orbitals (MO) of the free and physisorbed Crocin are similar. However, there are some differences in this case. The high occupied MO H-1 and H-2 Orbitals of Crocin in physisorbed structures are more delocalized than in the free one, favoring charge interactions, and resulting in three different adsorbed conformers of Crocin on the surface (Figure 11). Differences are also observed in the H-1, H-2 and other lowest in energy molecular orbitals when comparing free and physisorbed structures because of the increased planarity in the physisorbed one. For instance, comparing free Crocin and (a) physisorbed Crocin, the H-1 and H-2 MO of the (a) are more extended in the molecule.

Thereafter, the effectiveness of the inhibitor is correlated with the frontier MO, i.e., H, L, and mainly with the energy gap between them, E_L–E_H (Kathirvel et al. 2014; Martinez and Štagljar 2003; Verma et al. 2021). As mentioned above, the low E_L–E_H difference, i.e., 2.45 eV of Crocin (Table 4), and consequently the small hardness (η), shows its high capability for reaction. When Crocin is physisorbed on Al(110), the E_L–E_H difference remains the same, showing that its reactivity does not change. However, when it is physisorbed on Al_2O_3 surface, both the E_L–E_H difference and the hardness are reduced to half, showing that the reactivity is increased. Similarly, the E_{L+1}–E_H difference from 3.55 eV in free Crocin is reduced to 2.53 eV in physisorbed Crocin on Al_2O_3 surface, resulting in an increase

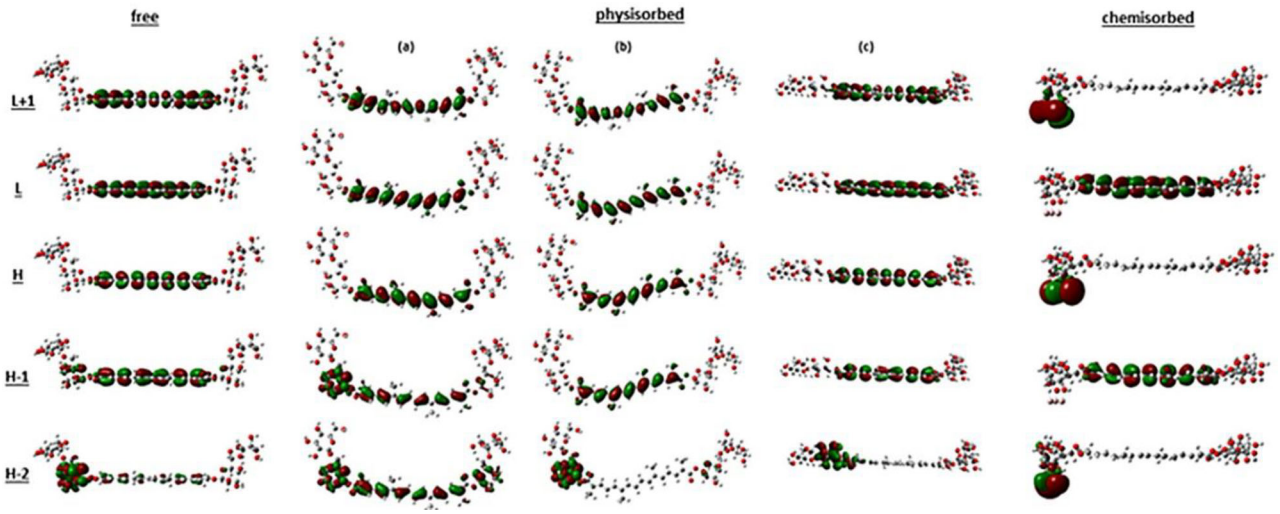

Figure 11. Frontier molecular orbitals of free, physisorbed (three different adsorbed structures) and chemisorbed Crocin molecule on Al_2O_3 surface.

Table 4. Relative energies in eV of the frontier molecular orbitals and hardness η (eV) of Crocin molecules and of the physisorbed or chemisorbed Crocin on Al_2O_3 and Al model cluster surfaces.

MO	Crocin	on Al_2O_3 surface				on Al surface	
		Phys[a] Large	Phys[a] Small model	Chem[a] Small model	Chem[a,b] Small model	Phys[a] Small model	Chem[a] Small model
L + 1	3.55	2.53	2.45	0.08	0.06	3.53	0.97
L	2.45	1.59	1.57	0.02	0.01	2.45	0.88
H	0.00	0.00	0.00	0.00	0.00	0.00	0.00
H-1	−1.05	−0.73	−0.90	−0.02	−0.15	−1.09	−1.54
H-2	−1.53	−0.75	−0.94	−0.07	−0.19	−1.43	−2.28
η	1.225	0.796	0.784	0.012	0.005	1.224	0.441

[a]Phys: physisorbed and Chem: chemisorbed.
[b]Charged surface.

in its reactivity when the L + 1 orbital is additionally involved in the reaction.

Chemisorption: The calculated E_L–E_H differences show a dramatic decrease in the case of chemisorption. Their values drop to about one third (compared to the physisorbed case) to become 0.88 eV in the case of Al(110) and by 120 times to 0.02 eV in the case of Al_2O_3 as shown in Table 4. Consequently, the value of hardness (η) is reduced also significantly of about 3 times (0.441/1.225) in the case of Al(110) and about 100 times (0.012/1.225) in the case of Al_2O_3, showing improved reactivity, i.e., formation of chemical bonds. The results indicate that the HOMO orbital of the system Crocin-surface has the electron density localized on the bonding, while the LUMO orbital of the system has the electron density on Crocin, showing that the electron excitation will be a charge transfer process.

Table 5. Bond distances R (Å) between Crocin and Al/Al_2O_3 surfaces at ONIOM(B3LYP/6-31G(d,p):UFF) and binding energies BE (eV) at B3LYP/6-31g(d,p) per molecule of Crocin.

	Al		Al_2O_3	
	R	BE	R	BE
Physisorbed Crocin	3.11	−0.08	2.40–2.79	−0.83
Chemisorbed Crocin[a]	1.55	−3.84	1.45–1.51	−4.68
Chemisorbed Crocin[a] & O_2	1.44			

[a]Chemisorbed Crocin forming one bond with the surface

Moreover, the fact that the H-2, H-1, H, L, L + 1 orbitals are close-lying means that electrons can more easily be transferred to the surfaces and thus enhance the chemical bonding of Crocin with the surfaces. Furthermore, it should be noted that the frontier molecular orbitals are more close-lying when attachment of Crocin occurs on Al_2O_3 than on Al, both in chemisorption and in physisorption on the surfaces, meaning that electrons can be transferred more easily. Thus, Crocin remains on the surface, despite the aqueous environment of this study, resulting in a good anti-corrosion performance, especially in the case of Al_2O_3.

Interaction Energies between Crocin and surfaces: The interaction energy, expressed as Binding Energy (BE), as well as the distances between Crocin and Al_2O_3 and Al surfaces were calculated (Figure 9 and Table 5). In the case of physisorption, BE is −0.08 eV on Al(110) and −0.83 eV on Al_2O_3 showing that the adsorption on Al_2O_3 is energetically more favorable, since the value of BE is 10 times higher than the adsorption on

Al(110). This occurs because OH … O van der Waals bonds are formed between the hydrogen atoms of Crocin and the oxygen atoms of the Al_2O_3 surface, leading the bond lengths to a range of 2.4 to 2.8 Å (Table 5). At these distances, the average interaction energy per van der Waals bond is less than 0.05 eV, revealing that in this case multiple interactions can be formed. However, the adsorption energy of Crocin on Al(110) is very small (-0.08 eV) and the distance from the surface is high (3.11 Å), showing that Crocin is very loosely attached and practically cannot remain on the surface of Al(110) if only physisorption occurs.

In the case of chemisorption, the Binding Energy (BE) values are −4.68 eV and −3.84 eV on Al_2O_3 and Al(110) respectively (Table 5). Accordingly, the bond distances become short (1.45 Å on Al_2O_3, and 1.55 Å on Al(110)), revealing strong chemical bond formation between Crocin molecules and both Al and Al_2O_3 surfaces. Besides, the examined bond distance of Crocin in O-vacancy positions of the Al_2O_3 surface and in Al-vacancy positions of Al(110), with or without removal of a H^+ cation from Crocin, becomes 1.44 Å. This fact confirms the spontaneous formation of oxide due to the instant bonding of O_2 and Al, when oxygen in the naturally aerated solution meets aluminum surface. Given the bond distances, chemical bond between Crocin and the point defect of the Al_2O_3 surface can be established.

In NaCl solution: Further theoretical calculations, show that both Na^+ and Cl^- ions interact with Crocin and Al_2O_3 surface forming Na^+ … O, Cl^- … Al, and Cl^- … H bonds (Figure 12 and Table 6). Stronger bonds between Na^+ and Crocin (BE −0.49 eV) than between Na^+ and Al_2O_3 surface (BE is −0.05 eV) are formed. In addition, calculations reveal that Cl^- ions form stronger bonds with Al_2O_3 surface (BE −0.69 eV) than with the H atoms of the OH groups of Crocin, where BE is only −0.09 eV.

The above results indicate that in a NaCl solution in the absence of Crocin, Cl^- are attracted to the Al_2O_3 surface, adsorbed in localized sites and penetrate into the oxide lattice, where they substitute O^{2-} creating also aluminum ion vacancies. In these conditions, the formation of soluble oxo-, hydro-, and chloro- complexes causes the passivity breakdown, retarding the film repairing, and accelerating pitting corrosion (Branzoi et al. 2003; Szklarska-Smialowska 1999; Liu et al. 2015). Liu and his coauthors (2015) using Density Functional Theory (DFT) found that Cl^- ions weaken the Al-O bond leading to breakdown of the passive layer, resulting to reduced protection, oxidation promotion and gradual dissolution of the aluminum surface. Simultaneously, AlO_2^- ions are formed probably due to a local increase in pH caused by the reduction of O_2, delaying also the repassivation of the surface (Oguzie et al. 2010). On the contrary, in the presence of Crocin this process is assumed to be restrained, due to multiple interactions between Crocin molecules and the Al_2O_3 surface. As a result, an almost complete coverage of the surface occurs minimizing its availability to corrosion and its dissolution by the aggressive solution. This is achieved firstly by planar orientation of Crocin molecules on the surface, with the internal glucose rings being at the same plane with the polyene chain, while the extreme ones being rotated due to H bonds with the carbonyl groups. Then Crocin molecules are chemisorbed on aluminum oxide through the hydroxyl groups of their sugar moiety, and in a lower degree via weak interactions on Al surface. This process is assisted by the π-conjugated system of the polyene chain together with the extended electron delocalization over the oxygen atoms of the esterified carboxyl groups. The easy rotation of C-C bonds of the glucose rings and their orientation contributes to the ability of the non-bonded OH groups in the extreme rings to face and repel the aggressive chloride ions of the solution and thus to protect the surface against corrosion. Moreover, even if chloride ions reach the aluminum oxide surface, the chemisorbed Crocin and its cation interact with corrosion products and principally with aluminate ions (AlO_2^-), healing the passive oxide layer immediately after corrosion initiation and blocking the corrosion process, as explained in the experimental part.

Finally, theoretical calculations were performed for the interactions of Crocin with negatively charged Al/Al_2O_3 surfaces, as can occur in the case of pH $>$ 7 or as a result of treatments or

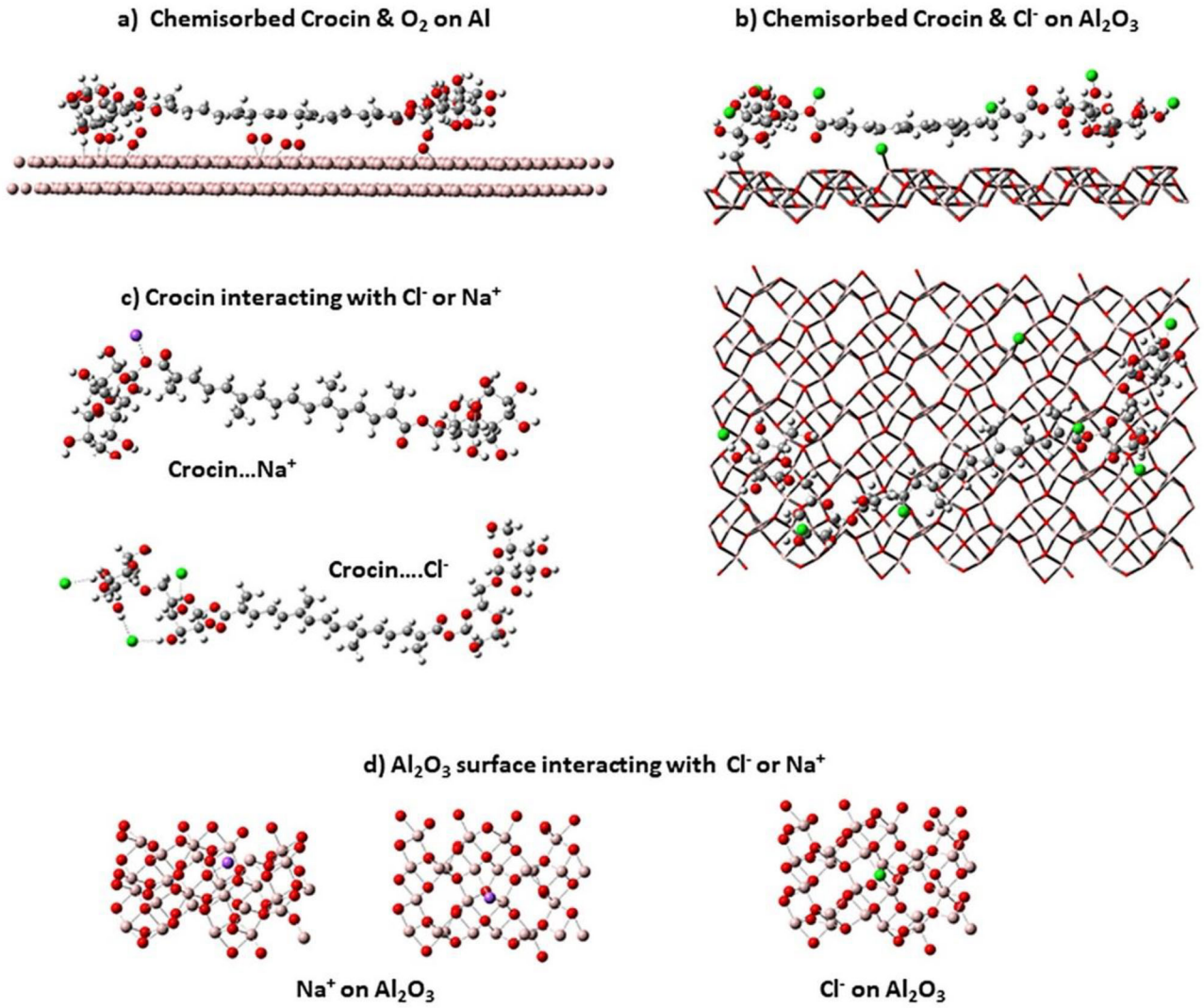

Figure 12. Calculated minimum structures of a) chemisorbed Crocin and O_2 on Al(110); b) chemisorbed Crocin and Cl^- anions on Al_2O_3 surface from two points of view; c) Crocin molecule interacting with Na^+ and Cl^- ions and d) Na^+ and Cl^- ions attached on Al_2O_3 surface.

Table 6. Bond distances R (Å) between Na^+ or Cl^- ions and Al_2O_3 surface or Crocin at B3LYP/6-31g(d,p) and PM6 levels of theory and binding energies BE (eV) per molecule of Crocin.

	R	BE
Cl^- … Al of Al_2O_3 surface	2.12–2.42	−0.69 (−6.94)[a]
Cl^- … .H of Crocin	2.17–2.27	−0.09
Na^+ … O of Al_2O_3 surface	2.91	−0.01
Na^+ … Al of Al_2O_3 surface	2.65–2.71	−0.05 (−5.69)[a]
Na^+ … O of Crocin	2.37–2.60	−0.49

[a]Chemisorbed Crocin forming one bond with the surface.

modifications of the surfaces, i.e., in alkaline solutions. It was found that the systems of chemisorbed Crocin-Al_2O_3 or Crocin-Al model surface clusters are further stabilized. This was established by employing B3LYP/6-31G(d,p) for a truncated system of Crocin-Al_2O_3 model surface cluster of 225 atoms and of Crocin-Al model surface cluster of 273 atoms at the geometry obtained via the large model surface clusters. For the Al model surface cluster, the Crocin-negatively charged surface is more stable than the neutral one by −4.4 eV when Crocin is physisorbed and by −5.1 eV when it is chemisorbed. For the Al_2O_3 model surface cluster, the Crocin-negatively charged surface is more stable than the neutral one by −3.5 eV when Crocin is physisorbed and by −4.1 eV when it is chemisorbed. This shows that the charge can be easily transferred to Crocin and that the system is further stabilized by about 0.6 eV. Additionally, it was found that binding energy between the chemisorbed Crocin and surface is higher in charged surface (> 0.1 eV) and as the charge of the surface increases, the binding energy increases too.

These findings could be the subject of future research on the possible interactions of Crocin molecules with charged surfaces of aluminum and aluminum oxide in various corrosive solutions.

Mechanism of inhibition: The above analysis reveals that initially Crocin is adsorbed physically on the aluminum oxide surface, deforming its minimum geometry in order to obtain a planar form and increase its interactions with the Al_2O_3 surface. This new geometry has an increased dipole moment about three times with respect to the equilibrium geometry, resulting in enhancement of chemical bonding with the Al atoms of the Al_2O_3 through the vicinal OH of the molecules of Crocin. This process is assisted by the electron donating character of Crocin due to the π-conjugated system of its polyene chain, which is extended to the carbonyls of the esterified groups of its molecules. Thus, Crocin remains attached on Al_2O_3, minimizing the available for corrosion surface and protecting it in the aggressive environment of chlorides. Moreover, the easy rotation of the C-C bonds of the glucose rings and the easy change of their orientation facilitate the non-bonded hydroxyls in the extreme rings to obstruct the approach of chlorides. Even if chloride ions manage to reach the aluminum oxide surface, the chemisorbed Crocin and its cation interact with corrosion products and mainly with aluminate ions (AlO_2^-) as soon as pitting corrosion starts, healing the passive oxide layer and blocking the corrosion process.

4. Conclusions

The role of Crocin as a green corrosion inhibitor for the AA 1050 commercial aluminum alloy in 0.01 M sodium chloride solution was investigated. Its action was assessed by Linear and Tafel Polarization, as well as by mass loss measurements and confirmed by observation and analysis of the specimen's surface morphology by SEM. Additionally, Crocin's inhibitive action was interpreted via theoretical calculations employing density functional theory, semiempirical PM6, molecular mechanics methodologies and ONIOM multiscaling approaches showing good agreement with experimental results. Conclusions and remarks from the results of this work are summarized below:

Crocin was proved to be a mixed-type green inhibitor with principally anodic inhibitive effect against aluminum corrosion in the aggressive environment of NaCl. Its anticorrosive action was found to improve as its concentration increases resulting in inhibition efficiency up to 95% obtained with the 1.25 mM solution of Crocin. Computational theoretical analysis for Crocin molecules and their interactions with Al_2O_3 showed that initially Crocin is physically adsorbed on the surface, deforming its minimum geometry in order to obtain a planar form and increase its interactions with the surface. Then the attachment of Crocin on the surface occurs preferably by chemisorption through chemical bonds due to the electron donating character of Crocin. The intense electrostatic potential regions located on the gentiobiose groups of Crocin could be the anchoring groups onto the positively charged passivated aluminum oxide surface. Thus, Crocin remains attached, creating a stable protective layer onto the surface in the corrosive environment, ensuring surface coverage, blocking the available sites of the surface for corrosive reactions and repulsing the aggressive chloride ions toward the solution. Moreover, at pitting corrosion sites Crocin interacts with the corrosion products, improving the healing of the oxide layer and the repassivation of the surface.

Acknowledgments

I. Tsangaraki-Kaplanoglou (NKUA, retired Assoc. Professor of Chemistry) is thanked for encouragement and theoretical discussions during the writing of this paper.

Funding

This research is co-financed by Greece and the European Union (European Social Fund- ESF) through the Operational Programme «Human Resources Development, Education and Lifelong Learning» in the context of the project "Reinforcement of Postdoctoral Researchers - 2nd Cycle" (MIS-5033021), implemented by the State Scholarships Foundation (IKY).

References

Abdallah M, Hawsawi H, Al-Gorair AS, Alotaibi MT, Al-Juaid SS, Hameed RSA. 2022. Appraisal of adsorption and inhibition effect of expired micardis drug on aluminum corrosion in hydrochloric acid solution. Int J Electrochem Sci. 17:Article ID:220462. doi:10.20964/2022.04.61.

Abdallah M, Gad EAM, Altass HM, El-Etre MA, Al Gorair AS, Al-Jahdaly BA, Al-Juaid SS. 2021. Inhibitive performance of dapoxetine drug for corrosion of aluminum alloy (AA6063) in acidic and alkaline solutions: experimental and theoretical studies using Materials Studio v7.0. DWT. 221:270–280. DOI: 10.5004/dwt.2021.27050.

Abdallah M, Awad MI, Altass HM, Morad M, El-Etre MA, Al-Fahemi JH, Sayed WM. 2020. Sildenafil drug as a safe anticorrosion for 6063 aluminum alloy in acidic and alkaline solutions: theoretical and experimental studies, Egypt. J. Pet. 29(3):211–218. 10.1016/j.ejpe.2020.06.001.

Akhtari K, Hassanzadeh K, Fakhraei B, Fakhraei N, Hassanzadeh H, Zarei SA. 2013. A density functional theory study of the reactivity descriptors and antioxidant behavior of Crocin. Comput Theor Chem. 1013:123–129. doi: 10.1016/j.comptc.2013.03.015.

Alexander M, Thompson GE, Beamson G. 2000. Characterization of the oxide/hydroxide surface of aluminium using X-ray photoelectron spectroscopy: a procedure for curve fitting the O 1s core level. Surf Interface Anal. 29(7):468–477. doi: 10.1002/1096-9918(200007)29:7.

Ambat R, Dwarakadasa ES. 1994. Studies on the influence of chloride ion and pH on the electrochemical behaviour of aluminium alloys 8090 and 2014. J Appl Electrochem. 24(9):911–916. doi: 10.1007/BF00348781.

Amitha Rani BE, Basu BBJ. 2012. Green inhibitors for corrosion protection of metals and alloys: An overview. Int J Corros. 2012:1–15. doi: 10.1155/2012/380217.

Ashassi-Sorkhabi H, Kazempour A. 2020. Chitosan, its derivatives and composites with superior potentials for the corrosion protection of steel alloys: a comprehensive review. Carbohydr Polym. 237:116110. doi: 10.1016/j.carbpol.2020.116110.

Aytaç A, Özmen Ü, Kabasakaloğlu M. 2005. Investigation of some Schiff bases as acidic corrosion of alloy AA3102. Mater Chem Phys. 89(1):176–181. doi:10.1016/j.matchemphys.2004.09.003.

Bathaie SZ, Farajzade A, Hoshyar R. 2014. A review of the chemistry and uses of crocins and crocetin, the carotenoid natural dyes in saffron, with particular emphasis on applications as colorants including their use as biological stains. Biotech Histochem. 89(6):401–411. doi: 10.3109/10520295.2014.890741.

Becke AD. 1993. A new mixing of Hartree-Fock and local density-functional theories. J Chem Phys. 98(2):1372–1377. doi:10.1063/1.464304.

Branzoi V, Golgovici F, Branzoi F. 2003. Aluminium corrosion in hydrochloric acid solutions and the effect of some organic inhibitors. Mater Chem Phys. 78(1):122–131. doi: 10.1016/S0254-0584(02)00222-5.

Byrne CE, D'Alessandro O, Deyá C. 2022. Tara tannins as a green sustainable corrosion inhibitor for aluminum. J Mater Eng Perform. 31(4):2918–2933. doi: 10.1007/s11665-021-06437-1.

Carneiro J, Tedim J, Ferreira M. 2015. Chitosan as a smart coating for corrosion protection of aluminum alloy 2024: a review. Prog Org Coat. 89:348–356. doi:10.1016/j.porgcoat.2015.03.008.

Cerdá-Bernad D, Valero-Cases E, Pastor JJ, Frutos MJ. 2022. Saffron bioactives crocin, crocetin and safranal: effect on oxidative stress and mechanisms of action. Crit Rev Food Sci Nutr. 62(12):3232–3249. doi: 10.1080/10408398.2020.1864279.

Costa D, Ribeiro T, Cornette P, Marcus P. 2016. DFT modeling of corrosion inhibition by organic molecules: carboxylates as inhibitors of aluminum corrosion. J Phys Chem C. 120(50):28607–28616. doi: 10.1021/acs.jpcc.6b09578.

Curtiss LA, McGrath MP, Blaudeau JP, Davis NE, Binning RC, Jr, Radom L. 1995. Extension of Gaussian-2 theory to molecules containing third-row atoms Ga–Kr. J Chem Phys. 103(14):6104–6113. doi: 10.1063/1.470438.

Dapprich S, Komáromi I, Byun KS, Morokuma K, Frisch MJ. 1999. A new ONIOM implementation in Gaussian98. Part I. The calculation of energies, gradients, vibrational frequencies and electric field derivatives. J Mol Struct Theochem. 461-462:1–21. doi: 10.1016/S0166-1280(98)00475-8.

De Proft F, Geerlings P. 2001. Conceptual and computational DFT in the study of aromaticity. Chem Rev. 101(5):1451–1464. doi: 10.1021/cr9903205.

El Mazyani A, Chafi M, Essahli M. 2021. Assessment of AA5005 aluminum alloy corrosion resistance by Direct Blue 15 inhibitor in sodium chloride medium. Mater Today. 37:3882–3888. doi: 10.1016/j.matpr.2020.08.473.

El-Etre AY. 2003. Inhibition of aluminum corrosion using Opuntia extract. Corros Sci. 45(11):2485–2495. doi: 10.1016/S0010-938X(03)00066-0.

Ezuber H, El-Houd A, El-Shawesh F. 2008. A study on the corrosion behavior of aluminum alloys in seawater. Mater Des. 29(4):801–805. doi: 10.1016/j.matdes.2007.01.021.

Fernine Y, Ech-Chihbi E, Arrousse N, El Hajjaji F, Bousraf F, Ebn Touhami M, Rais Z, Taleb M. 2021. Ocimum basilicium seeds extract as an environmentally friendly antioxidant and corrosion inhibitor for aluminium alloy 2024 -T3 corrosion in 3 wt% NaCl medium. Colloids Surf A Physicochem Eng Asp. 627:127232. doi: 10.1016/j.colsurfa.2021.127232.

Fouda AS, Al-Sarawy AA, Ahmed FS, El-Abbasy HM. 2009. Corrosion inhibition of aluminum 6063 using some pharmaceutical compounds. Prot Met Phys Chem Surf. 45(5):635–643. doi: 10.1134/S2070205109050244.

Frisch MJ, Trucks GW, Schlegel HB, Scuseria GE, Robb MA, Cheeseman JR, Scalmani G, Barone V, Petersson GA, Nakatsuji H. 2016. Gaussian 16, Revision C.01. Wallingford (CT): Gaussian, Inc.

Garrigues L, Pebere N, Dabosi F. 1996. An investigation of the corrosion inhibition of pure aluminum in neutral and acidic chloride solutions. Electrochim Acta. 41(7-8): 1209–1215. doi: 10.1016/0013-4686(95)00472-6.

Giles CH. 1974. The coloration of aluminium. Rev Prog Coloration. 5(1):49–64. doi: 10.1111/j.1478-4408.1974.tb03790.x.

Kasprzyk-Hordern B. 2004. Chemistry of alumina, reactions in aqueous solution and its application in water treatment. Adv Colloid Interface Sci. 110(1-2):19–48. doi: 10.1016/j.cis.2004.02.002.

Kathirvel K, Thirumalairaj B, Jaganathan M. 2014. Quantum chemical studies on the corrosion inhibition of mild steel by piperidin-4-one derivatives in 1 M H_3PO_4. OJMetal. 04(04):73–85. doi: 10.4236/ojmetal.2014.44009.

Kliškić M, Radoševic' J, Gudic' S. 1997. Pyridine and its derivatives as inhibitors of aluminium corrosion in chloride solution. J Appl Electrochem. 27(8):947–952. doi: 10.1023/A:1018405803182.

Kummert R, Stumm W. 1980. The surface complexation of organic acids on hydrous γ-Al_2O_3. J Colloid Interface Sci. 75(2):373–385. doi: 10.1016/0021-9797(80)90462-2.

Lai X, Hu J, Ruan T, Zhou J, Qu J. 2021. Chitosan derivative corrosion inhibitor for aluminum alloy in sodium chloride solution: a green organic/inorganic hybrid. Carbohydr Polym. 265:118074. doi: 10.1016/j.carbpol.2021.118074.

Lee C, Yang W, Parr RG. 1988. Development of the Colle-Salvetti correlation energy formula into a functional of the electron density. Phys Rev B Condens Matter. 37(2): 785–789. doi: 10.1103/PhysRevB.37.785.

Lee EJ, Pyun SI. 1995. The effect of oxide chemistry on the passivity of aluminium surfaces. Corros Sci. 37(1): 157–168. doi: 10.1016/0010-938X(94)00127-R.

Liu M, Jin Y, Zhang C, Leygraf C, Wen L. 2015. Density-functional theory investigation of Al pitting corrosion in electrolyte containing chloride ions. Appl Surf Sci. 357(1):2028–2038. doi: 10.1016/j.apsusc.2015.09.180.

Luo X, Ci C, Li J, Lin K, Du S, Zhang H, Li X, Cheng YF, Zang J, Liu Y. 2019. 4-aminoazobenzene modified natural glucomannan as a green eco-friendly inhibitor for the mild steel in 0.5 M HCl solution. Corros Sci. 151: 132–142. doi: 10.1016/j.corsci.2019.02.027.

Ma F-Y. 2012. Corrosive effects of chlorides on metals. In: Nasr Bensalah, editor. Pitting Corrosion. IntechOpen. p. 139–178. doi: 10.5772/32333.

Maayta AK, Al-Rawashdeh NAF. 2004. Inhibition of acidic corrosion of pure aluminum by some organic compounds. Corros Sci. 46(5):1129–1140. doi: 10.1016/j.corsci.2003.09.009.

Martinez S, Štagljar I. 2003. Correlation between the molecular structure and the corrosion inhibition efficiency of chestnut tannin in acidic solutions. J Mol Struct Theochem. 640(1–3):167–174. doi:10.1016/j.theochem.2003.08.126.

McCafferty E. 2003. Sequence of steps in the pitting of aluminum by chloride ions. Corros Sci. 45(7):1421–1438. doi: 10.1016/S0010-938X(02)00231-7.

Müller B. 2002. Corrosion inhibition of aluminium and zinc pigments by saccharides. Corros Sci. 44(7):1583–1591. doi: 10.1016/S0010-938X(01)00170-6.

Murer N, Buchheit RG. 2013. Stochastic modeling of pitting corrosion in aluminum alloys. Corros Sci. 69:139–148. doi: 10.1016/j.corsci.2012.11.034.

Nakashima PNH. 2018. The crystallography of aluminum and its alloys. In: The encyclopedia of aluminum and its alloys. Boca Raton (FL): Chapman and Hall/CRC. p. 488–586. doi: 10.1201/9781351045636-140000245.

Natishan PM, O'Grady WE. 2014. Chloride ion interactions with oxide-covered aluminum leading to pitting corrosion: a review. J Electrochem Soc. 161(9):C421–C432. doi: 10.1149/2.1011409jes.

Obot IB, Macdonald DD, Gasem ZM. 2015. Density functional theory (DFT) as a powerful tool for designing new organic corrosion inhibitors. Part 1: an overview. Corros Sci. 99:1–30. doi: 10.1016/j.corsci.2015.01.037.

Oguzie EE. 2007. Corrosion inhibition of aluminium in acidic and alkaline media by Sansevieria trifasciata extract. Corros Sci. 49(3):1527–1539. doi: 10.1016/j.corsci.2006.08.009.

Oguzie EE, Akalezi CO, Enenebeaku CK, Aneke JN. 2010. Corrosion inhibition and adsorption behavior of malachite green dye on aluminum corrosion. Chem Eng Comm. 198(1):46–60. doi: 10.1080/00986445.2010.493118.

Oguzie EE, Okolue BN, Ogukwe C, Unaegbu C. 2006. Corrosion inhibition and adsorption behaviour of bismark brown dye on aluminium in sodium hydroxide solution. Mater Lett. 60(28):3376–3378. doi:10.1016/j.matlet.2006.03.018.

Omelchenko IV, Shishkin OV, Gorb L, Leszczynski J, Fias S, Bultinck P. 2011. Aromaticity in heterocyclic analogues of benzene: comprehensive analysis of structural aspects, electron delocalization and magnetic characteristics. Phys Chem Chem Phys. 13(46):20536–20548. doi: 10.1039/C1CP20905A.

Önal AN, Aksüt AA. 2000. Corrosion inhibition of aluminium alloys by tolyltriazole in chloride solutions. Anti-Corros Method M. 47(6):339–349. doi: 10.1108/00035590010354177.

Pantazopoulou P, Theohari S, Kalogeropoulou S. 2021. Organic dyes as corrosion inhibitors of commercial AA1050 aluminum alloy in sodium chloride environment. MATEC Web of Conference 349, 02017, ICEAF-VI, 2021. doi: 10.1051/matecconf/202134902017.

Pearson RG. 1993. The principle of maximum hardness. Acc Chem Res. 26(5):250–255. doi: 10.1021/ar00029a004.

Proença CS, Serrano B, Correia J, Machado Araújo ME. 2022. Evaluation of tannins as potential green corrosion inhibitors of aluminium alloy used in aeronautical industry. Metals. 12(3):508. doi: 10.3390/met12030508.

Rahaiee S, Moini S, Hashemi M, Shojaosadati SA. 2015. Evaluation of antioxidant activities of bioactive

compounds and various extracts obtained from saffron (*Crocus sativus* L.): a review. J Food Sci Technol. 52(4): 1881–1888. doi: 10.1007/s13197-013-1238-x.

Raja PB, Sethuraman MG. 2008. Natural products as corrosion inhibitor for metals in corrosive media – a review. Mater Lett. 62(1):113–116. doi: 10.1016/j.matlet.2007.04.079.

Rakshit A, Bandyopadhyay P, Heindel JP, Xantheas SS. 2019. Atlas of putative minima and low-lying energy networks of water clusters n = 3–25. J Chem Phys. 151(21): 214307. doi: 10.1063/1.5128378.

Rappé AK, Casewit CJ, Colwell KS, Goddard IW, Skiff WM. 1992. UFF, a full periodic-table force-field for molecular mechanics and molecular dynamics simulations. J Am Chem Soc. 114(25):10024–10035. doi: 10.1021/ja00051a040.

Rocher-Casterline BE, Ch'ng LC, Mollner AK, Reisler H. 2011. Communication: determination of the bond dissociation energy (D0) of the water dimer, $(H_2O)_2$, by velocity map imaging. J Chem Phys. 134(21):211101. doi: 10.1063/1.3598339.

Rosliza R, Nora'aini A, Wan Nik WB. 2010. Study on the effect of vanillin on the corrosion inhibition of aluminum alloy. J Appl Electrochem. 40(4):833–840. doi: 10.1007/s10800-009-0066-1.

Sangeetha M, Rajendran S, Sathiyabamaa J, Krishnavenic A. 2013. Inhibition of corrosion of aluminium and its alloys by extracts of green inhibitors. Port Electrochim Acta. 31(1):41–52. doi: 10.4152/pea.201301041.

Sheasby PG, Wernick S, Pinner R. 1987. Surface treatment and finishing of aluminum and its alloys. Vol. 1 and 2, 5th ed. Metals Park (OH): ASM International and Teddington, Middlesex (UK): Finishing Publications Ltd.

Solmaz R, Kardaş G, Yazıcı B, Erbil M. 2008. Citric acid as natural corrosion inhibitor for aluminium protection. Corros Eng Sci Technol. 43(2):186–191. doi: 10.1179/174327807X214770.

Soror TY. 2013. Saffron extracts as environmentally safe corrosion inhibitors for aluminium dissolution in 2M HCl solution. Eur Chem Bull. 2(4):191–196. doi:10.17628/ECB.2013.2.191-196.

Spencer MJS, Nyberg GL. 2002. DFT modelling of hydrogen on Cu(110)- and (111)-type clusters. Mol Simul. 28(8–9): 807–825. doi: 10.1080/0892702021000002502.

Stewart JJP. 2007. Optimization of parameters for semiempirical methods V: modification of NDDO approximations and application to 70 elements. J Mol Model. 13(12):1173–1213. doi: 10.1007/s00894-007-0233-4.

Szklarska-Smialowska Z. 1999. Pitting corrosion of aluminum. Corros Sci. 41(9):1743–1767. doi: 10.1016/S0010-938X(99)00012-8.

Theohari S, Kanta A, Tsangaraki I. 2015. Chemical etching of aluminum as a pretreatment improving the anti-corrosive properties of certain organic compounds. Proceedings of 4th International Conference of Engineering Against Failure, 2015 Jun 24–26; Skiathos, Greece.

Tirbonod F, Fiaud C. 1978. Inhibition of the corrosion of aluminium alloys by organic dyes. Corros Sci. 18(2): 139–149. doi: 10.1016/S0010-938X(78)80084-5.

Tsangaraki-Kaplanoglou I, Kanta A, Theohari S, Ninni V. 2010. Acid-dyes as corrosion inhibitors for mechanically pretreated aluminum. Anti-Corros Method M. 57(1): 6–12. doi: 10.1108/00035591011009673.

Tsangaraki-Kaplanoglou I, Moshohoritou R, Kallithrakas-Kontos N. 1989. The use of a natural dye in the formation of a thin coloured coating on an aluminium surface. J Soc Dye Colour. 105(3):114–119. doi: 10.1111/j.1478-4408.1989.tb01201.x.

Tsirelson VG, Antipin M, Gerr RG, Ozerov RP, Struchkov Y. 1985. Ruby structure peculiarities derived from X-ray diffraction data localization of chromium atoms and electron deformation density. Phys Stat Sol (A). 87(2): 425–433. doi: 10.1002/pssa.2210870204.

Tzeli D, Mavridis A, Xantheas SS. 2002. First principles examination of the acetylene-water clusters, HCCH-(H_2O)x, x = 2, 3, and 4. J Phys Chem A. 106(46): 11327–11337. doi: 10.1021/jp021191q.

Umoren SA, AlAhmary AA, Gasem ZM, Solomon MM. 2018. Evaluation of chitosan and carboxymethyl cellulose as eco-friendly corrosion inhibitors for steel. Int J Biol Macromol. 117:1017–1028. doi: 10.1016/j.ijbiomac.2018.06.014.

Verma C, Ebenso EE, Bahadur I, Quraishi MA. 2018. An overview on plant extracts as environmental sustainable and green corrosion inhibitors for metals and alloys in aggressive corrosive media. J Mol Liq. 266:577–590. doi: 10.1016/j.molliq.2018.06.110.

Verma C, Ebenso EE, Quraishi MA, Hussain CM. 2021. Recent developments in sustainable corrosion inhibitors: design, performance and industrial scale applications. Mater Adv. 2(12):3806–3850. doi: 10.1039/D0MA00681E.

Vreven T, Morokuma K. 2006. Chapter 3 hybrid methods: ONIOM(QM:MM) and QM/MM. Ann Rep Comput Chem. 2:35–51. doi: 10.1016/S1574-1400(06)02003-2.

Nik WBW, Zulkifli F, Sulaiman O, Samo KB, Rosliza R. 2012. Study of Henna (*Lawsonia inermis*) as natural corrosion inhibitor for aluminum alloy in seawater. IOP Conf Ser: Mater Sci Eng. 36:012043. doi: 10.1088/1757-899X/36/1/012043.

Xhanari K, Finsgar M. 2019. Organic corrosion inhibitors for aluminum and its alloys in chloride and alkaline solutions: a review. Arab J Chem. 12(8):4646–4663. doi: 10.1016/j.arabjc.2016.08.009.

Xhanari K, Finšgar M, Knez Hrnčič M, Maver U, Knez Ž, Seiti B. 2017. Green corrosion inhibitors for aluminium and its alloys: a review. RSC Adv. 7(44):27299–27330. doi: 10.1039/C7RA03944A.

Yan X, Hong L, Pei S, Hamilton A, Sun H, Yang R, Liu A, Yang L. 2021. A natural yellow colorant from *Buddleja officinalis* for dyeing hemp fabric. Ind Crops Prod. 171: 113968. doi: 10.1016/j.indcrop.2021.113968.

Zhang K, Yang W, Xu B, Chen Y, Yin X, Liu Y, Zuo H. 2018. Inhibitory effect of konjac glucomanan on pitting corrosion of AA5052 aluminium alloy in NaCl solution. J Colloid Interface Sci. 517:52–60. doi: 10.1016/j.jcis.2018.01.092.